

Effect of phase transformation on the converse magnetoelectric properties of a heterostructure of $\text{Ni}_{49.2}\text{Mn}_{29.6}\text{Ga}_{21.2}$ and $0.7\text{PbMg}_{1/3}\text{Nb}_{2/3}\text{O}_3\text{-}0.3\text{PbTiO}_3$ crystals

M. Zeng,^{1,2} Siu Wing Or,^{2,a)} and Helen Lai Wa Chan¹

¹Department of Applied Physics, The Hong Kong Polytechnic University, Hung Hom, Kowloon, Hong Kong

²Department of Electrical Engineering, The Hong Kong Polytechnic University, Hung Hom, Kowloon, Hong Kong

(Received 6 February 2010; accepted 2 April 2010; published online 6 May 2010)

We report experimentally and theoretically the effect of phase transformation on the converse magnetoelectric (CME) properties of a heterostructure formed by one layer of piezoelectric $0.7\text{PbMg}_{1/3}\text{Nb}_{2/3}\text{O}_3\text{-}0.3\text{PbTiO}_3$ (PMN-PT) crystal sandwiched between two layers of ferromagnetic shape memory $\text{Ni}_{49.2}\text{Mn}_{29.6}\text{Ga}_{21.2}$ (Ni-Mn-Ga) crystal. The CME coefficient (α_B) of the heterostructure remains minimally and relatively constant in the martensitic phase ($<28^\circ\text{C}$), attains its maximum value in the martensitic-austenitic phase transformation ($28\text{--}39^\circ\text{C}$), and decreases gradually with increasing temperature in the austenitic phase ($>39^\circ\text{C}$). Giant resonance α_B of 18.6 G/V is found at 32°C under a very low bias magnetic field of 150 Oe. © 2010 American Institute of Physics. [doi:10.1063/1.3427388]

Electric field-induced magnetization, called converse magnetoelectric (CME) effect, has attracted considerable interest due to the potential application in innovative electric-write high-density data storages.^{1–8} In single-phase multiferroics, such as perovskite BiFeO_3 and TbMn_2O_5 ,^{1,2} the CME effect arises from the intrinsic coupling between electric and magnetic dipoles at atomic scale is generally weak and only obtainable at low temperatures. In multiphase composites, the CME effect due to the product of the converse piezoelectric effect in piezoelectric materials (e.g., $\text{PbMg}_{1/3}\text{Nb}_{2/3}\text{O}_3\text{-PbTiO}_3$ (PMN-PT) crystal, $\text{Pb}(\text{Zr}_{1-x}\text{Ti}_x)\text{O}_3$ (PZT) ceramics, etc.) and the converse magnetostrictive effect in magnetostrictive materials [e.g., $\text{Tb}_{0.3}\text{Dy}_{0.7}\text{Fe}_{1.92}$ (Terfenol-D) alloy] is much stronger and can be characterized by the CME coefficient (α_B) defined as a magnetic induction in response to an applied ac electric voltage ($\alpha_B = dB/dV$).^{3–8}

To obtain a high CME effect in the composites, the magnetic component in the composites should have a strong coupling between elastic and magnetic domains.³ Recently, ferromagnetic shape memory Ni-Mn-Ga single crystals were found to exhibit both ferromagnetic and ferroelastic ordering simultaneously.⁹ As a result, they have magnetoelastic coupling which makes them possible to manipulate their ferroelastic domains by an applied magnetic field or mechanical stress. Many studies have been made on the magnetic response to external mechanical stimulus (strain/stress) in Ni-Mn-Ga crystals,^{9–14} e.g., Li *et al.*¹² reported a change in magnetization of 540 G under stress training of 3.5 MPa. These studies present a strong sensing effect in the change in magnetization with respect to the external mechanical stimulus, and mean that Ni-Mn-Ga crystals have potential advantage in devoting the magnetic component to multiphase CME composites to achieve a large CME effect. Thus, in this work, we aim to study the CME effect in a heterostructure

consisting of a PMN-PT crystal plate bonded between two Ni-Mn-Ga crystal plates. Concentration is put on the effect of phase transformation in the Ni-Mn-Ga crystal plates on the resulting CME effect in the heterostructure.

Figure 1(a) shows the schematic diagram of the proposed heterostructure fabricated by bonding one layer of piezoelectric PMN-PT crystal plate between two layers of ferromagnetic shape memory Ni-Mn-Ga crystal plates. The two Ni-Mn-Ga plates, with a chemical composition of $\text{Ni}_{49.2}\text{Mn}_{29.6}\text{Ga}_{21.2}$, dimensions of $11 \times 5 \times 0.5 \text{ mm}^3$, and the two major surfaces parallel to the $\{011\}$ plane, were supplied

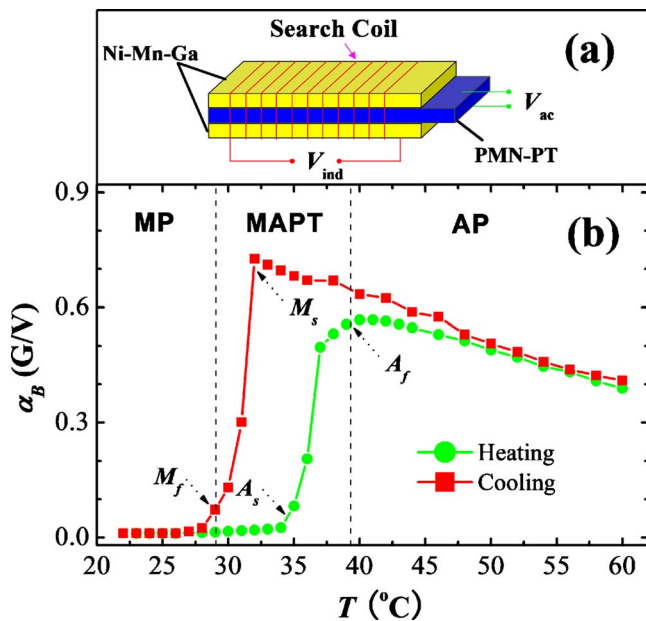


FIG. 1. (Color online) (a) Schematic diagram of the proposed heterostructure. The yellow (or lighter) blocks denote the Ni-Mn-Ga crystal plates, while the blue (or darker) block represents the PMN-PT plate. (b) CME coefficient (α_B) dependence on temperature (T) at an applied ac electric voltage (V_{ac}) of 20 V (peak), a frequency (f) of 1 kHz, and a magnetic bias field (H_{Bias}) of 150 Oe upon heating and cooling.

^{a)}Author to whom correspondence should be addressed. Electronic mail: esewor@polyu.edu.hk.

by AdaptaMat Ltd. in Finland. The PMN-PT plate, having a chemical composition of $0.7\text{PbMg}_{1/3}\text{Nb}_{2/3}\text{O}_3\text{-}0.3\text{PbTiO}_3$, dimensions of $12 \times 5 \times 0.8$ mm³, an electric polarization along its thickness in the (001) direction, and piezoelectric d_{31} and d_{33} coefficients of -2500 pC/N and 2000 pC/N, respectively, was provided by Shanghai Institute of Ceramics, Chinese Academy of Sciences in China.

To acquire the induced magnetic induction (B_{ind}), a search coil with 30 turns of Cu wire was wrapped around the heterostructure, and the whole heterostructure-search coil assembly was immersed in a temperature (T)-controlled silicone oil bath placed in the middle of the pole gap of an electromagnet (MyItem PEM-8005K). By energizing the electromagnet with a dc current supply (Sorenson DHP200-15), a magnetic bias field (H_{Bias}) was generated in the pole gap along the length direction of the heterostructure. A Hall probe connected to a Gaussmeter (F. W. Bell 7030) and situated adjacent to the heterostructure was used to monitor H_{Bias} . An arbitrary function generator (AFG310) connected to a power-supply amplifier (Techron TEC7572) was employed to provide an applied ac electric voltage (V_{ac}) at a prescribed frequency (f) to the PMN-PT plate of the heterostructure. The change in magnetic flux associated with the Ni-Mn-Ga plates due to the applied V_{ac} to the PMN-PT plate led to an induced voltage (V_{ind}) in the search coil [Fig. 1(a)]. By integrating this V_{ind} with respect to time using an integrating fluxmeter (Walker LDJ MF-10D), the corresponding magnetic induction (B_{ind}) from the Ni-Mn-Ga plates was measured by a dynamic signal analyzer (Ono Sokki CF5220). In the present study, the CME coefficient expressed by $\alpha_B = dB_{\text{ind}}/dV_{\text{ac}}$ was evaluated under different combinations of temperature (T), magnetic bias field (H_{Bias}), and frequency (f).

Figure 1(b) shows the α_B dependence on T at $V_{\text{ac}} = 20$ V (peak), $f = 1$ kHz, and $H_{\text{Bias}} = 150$ Oe upon heating and cooling. It is clear that the CME effect depends greatly on T . The heating and cooling curves form an obvious hysteresis loop with a temperature hysteresis of about 5 °C. The four critical transformation temperatures are found to be austenite start $A_s = 35$ °C, austenite finish $A_f = 39$ °C, martensite start $M_s = 32$ °C, and martensite finish $M_f = 28$ °C. The hysteresis loop, as a whole, can be divided into three distinct regions, representing the martensitic phase (MP) (<28 °C), martensitic-austenitic phase transformation (MAPT) (28–39 °C), and austenitic phase (AP) (>39 °C), to be described as follows.

In MP, it is noted that the Ni-Mn-Ga plates exhibit a giant twin-variant reorientation strain (=5.6% in our samples) under an external magnetic field or mechanical stress. The twin-variant motion is mainly responsible for the change in magnetization.¹¹ Since the elastic modulus of Ni-Mn-Ga plates at twin-variant motion (~ 30 MPa) (Ref. 17)⁷ is much smaller than that of PMN-PT plate (~ 280 GPa), the strain in the Ni-Mn-Ga plates can be assumed to follow that in the PMN-PT plate. Thus, the electric field-induced change in magnetic induction can be expressed as:¹⁴

$$B_{\text{ind}} = \frac{d_{31} \times V_{\text{ac}}}{\varepsilon_0 \times t_p} \Delta B_S = \alpha_B V_{\text{ac}}, \quad (1)$$

where d_{31} (=−2500 pC/N) is the piezoelectric coefficient, t_p (=0.8 mm) is the thickness of the PMN-PT plate,

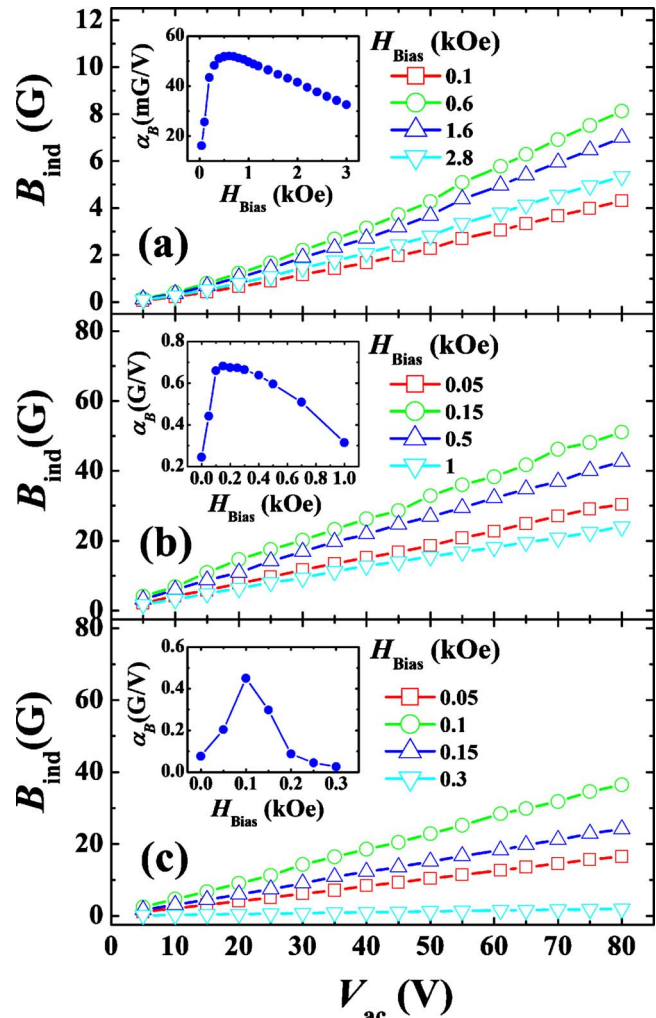


FIG. 2. (Color online) Magnetic induction (B_{ind}) as a function of applied ac electric voltage (V_{ac}) for various magnetic bias fields (H_{Bias}) at a frequency (f) of 1 kHz in (a) MP (at 25 °C), (b) MAPT (at 32 °C), and (c) AP (at 50 °C). The insets show the variations in CME coefficient (α_B) with H_{Bias} obtained from the slopes of the $B_{\text{ind}}-V_{\text{ac}}$ plots at different H_{Bias} .

ε_0 (=6%) is the theoretical maximum lattice strain of Ni-Mn-Ga plates, and ΔB_S (=0.12 T) (Ref. 14) is the maximum change in magnetic induction upon a full reorientation of twin variants at a given H_{Bias} . From Eq. (1), α_B is estimated to be 62.4 mG/V, which is in good agreement with the experimental value shown in the inset of Fig. 2(a). It is the twin-variant motion so that α_B is relatively small and constant for T below 28 °C.

In MAPT, one distinct property is the abrupt change in magnetization at nonsaturation field levels.¹⁵ The piezoelectric strain generated from the PMN-PT plate, upon transferring to the Ni-Mn-Ga plates, leads to phase transformation. Hence, the CME effect is mainly due to the electric field-induced MAPT and is proportional to the difference in magnetization between MP and AP. It also results in the maximization of the CME effect.^{8,11}

In AP, α_B decreases gradually with increasing T above 39 °C. This is mainly due to the absence of twin variants so that the strain drops dramatically. The stress effect at the interfaces is responsible for the variation in magnetic induction. Similar to traditional magnetostrictive materials such as Terfenol-D, α_B can be expressed as follows:^{6,11,16}

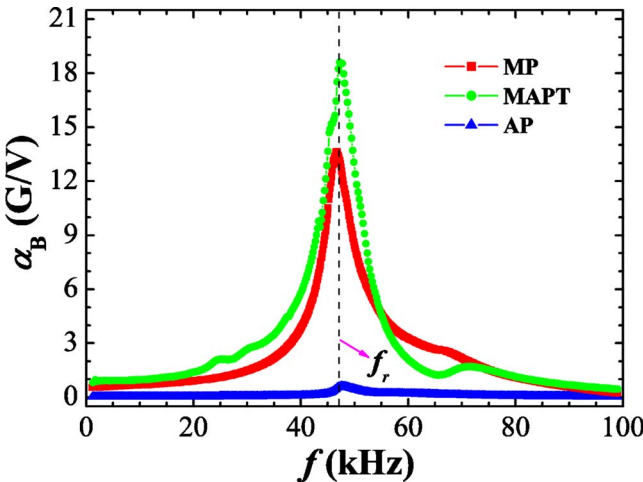


FIG. 3. (Color online) CME coefficient (α_B) as a function of frequency (f) at an applied ac electric voltage (V_{ac}) of 20 V (peak) and a magnetic bias field (H_{Bias}) of 150 Oe in MP (at 25 °C), MAPT (at 32 °C), and AP (at 50 °C).

$$B_{ind} \cong \frac{3}{2} \frac{\lambda_S \sigma_P t_P}{M_S t_n} = \frac{3}{2} \frac{\lambda_S Y d_{31} V_{ac}}{M_S t_n} = \alpha_B \times V_{ac}, \quad (2)$$

where λ_S (=−640 ppm at 50 °C), M_S (=0.56 T at 50 °C), σ_p , and t_n (=1 mm) are the saturation strain, saturation magnetization, induced stress, and thickness of the Ni–Mn–Ga plates, respectively, and Y (=280 GPa) and t_p (=0.8 mm) are the Young's modulus and thickness of PMN-PT plate, respectively. It is noted that $\partial\lambda/\partial M$ is greatly dependent on H_{Bias} .⁷ The calculated α_B , based on Eq. (2), in fact, is the average value and estimated to be 0.12 G/V, which is consistent with the average experimental value shown in the inset of Fig. 2(c).

Figure 2 plots the B_{ind} as a function of applied V_{ac} for various H_{Bias} at f of 1 kHz in MP (at 25 °C) [Fig. 2(a)], MAPT (at 32 °C) [Fig. 2(b)], and AP (at 50 °C) [Fig. 2(c)]. It is seen that B_{ind} has good linear responses to V_{ac} in the entire V_{ac} range of 5–80 V (peak) for all H_{Bias} . Specifically, the greatest B_{ind} - V_{ac} response occurs at H_{Bias} =600 Oe, 150 Oe, and 100 Oe for MP, MAPT, and AP, respectively. The insets show the variations in CME coefficient (α_B) with H_{Bias} as obtained from the slopes of the B_{ind} - V_{ac} plots at different H_{Bias} . For all the three cases, α_B increases initially, reaching the maximum value and then decreasing with increasing H_{Bias} . The maximum α_B are 0.052, 0.68, and 0.54 G/V at H_{Bias} =600 Oe, 150 Oe, and 100 Oe in MP, MAPT, and AP, respectively.

Figure 3 shows the α_B as a function of f at an applied V_{ac} of 20 V (peak) and H_{Bias} of 150 Oe in MP (at 25 °C), MAPT (at 32 °C), and AP (at 50 °C). For all cases, a remarkable

resonance peak, located at about 47 kHz, is observed, indicating the fundamental electromechanomagnetic resonance of the heterostructure. Particularly, a giant resonance α_B of 18.6 G/V is detected at 32 °C in MAPT. This α_B is also the maximum α_B reported to date as expected by the author in Ref. 8. It is noted from Fig. 3 that the full width at half maximum of the resonance peak associated with MAPT (at 32 °C) is as large as 17 kHz, which is much larger than that of the previous report.¹¹

In summary, a heterostructure has been developed by sandwiching one piezoelectric PMN-PT plate between two ferromagnetic shape memory Ni–Mn–Ga plates. A giant resonance α_B of 18.6 G/V, which is the maximum reported value to date, has been observed in MAPT under a very low H_{Bias} of 150 Oe. The result paves a way for promising applications of the heterostructure in transducers, sensors, and electrically controlled magnetic memory devices.

This work was supported by the Hong Kong Research Grants Council of the HKSAR Government (Grant No. PolyU5257/06E) and The Hong Kong Polytechnic University (Grant Nos. A-PA3C and 1-BB95). The authors also thank Professor Haosu Luo of Shanghai Institute of Ceramics, Chinese Academy of Sciences for the supply of PMN-PT single crystal.

- ¹N. Hur, S. Park, P. A. Sharma, J. S. Ahn, S. Guha, and S.-W. Cheong, *Nature (London)*, **429**, 392 (2004).
- ²Y. H. Chu, L. W. Martin, M. B. Holcomb, M. Gajek, S. J. Han, Q. He, N. Balke, C. H. Yang, D. Lee, W. Hu, Q. Zhan, P. L. Yang, A. F. Rodríguez, A. Scholl, S. X. Wang, and R. Ramesh, *Nat. Mater.*, **7**, 478 (2008).
- ³J. G. Wan, J. M. Liu, G. H. Wang, and C. W. Nan, *Appl. Phys. Lett.*, **88**, 182502 (2006).
- ⁴Y. M. Jia, S. W. Or, H. L. W. Chan, X. Y. Zhao, and H. S. Luo, *Appl. Phys. Lett.*, **88**, 242902 (2006).
- ⁵C. Popov, H. Chang, P. M. Record, E. Abraham, R. W. Whatmore, and Z. Huang, *J. Electroceram.*, **20**, 53 (2008).
- ⁶Y. Chen, J. Wang, M. Liu, J. Lou, N. X. Sun, C. Vittoria, and V. G. Harris, *Appl. Phys. Lett.*, **93**, 112502 (2008).
- ⁷Y. M. Jia, F. F. Wang, X. Y. Zhao, H. S. Luo, S. W. Or, and H. L. W. Chan, *Compos. Sci. Technol.*, **68**, 1440 (2008).
- ⁸S. Y. Chen, D. H. Wang, Z. D. Han, C. L. Zhang, Y. W. Du, and Z. G. Huang, *Appl. Phys. Lett.*, **95**, 022501 (2009).
- ⁹P. Müllner, V. A. Chernenko, and G. Kostorz, *Scr. Mater.*, **49**, 129 (2003).
- ¹⁰I. Suorsa, E. Pagounis, and K. Ullakko, *Appl. Phys. Lett.*, **84**, 4658 (2004).
- ¹¹S. Kustov, F. Masdeu, and E. Cesari, *Appl. Phys. Lett.*, **89**, 061917 (2006).
- ¹²G. Li and Y. Liu, *Appl. Phys. Lett.*, **88**, 232504 (2006).
- ¹³I. Karaman, B. Basaran, and H. E. Karaca, *Appl. Phys. Lett.*, **90**, 172505 (2007).
- ¹⁴N. N. Sarawate and M. Dapino, *Appl. Phys. Lett.*, **93**, 062501 (2008).
- ¹⁵V. A. Chernenko, V. A. L'vov, and E. Cesari, *J. Magn. Magn. Mater.*, **196**, 859 (1999).
- ¹⁶M. J. Sablik, S. W. Rubin, L. A. Riley, D. C. Jiles, D. A. Kaminski, and S. B. Biner, *J. Appl. Phys.*, **74**, 480 (1993).
- ¹⁷E. Gans and G. P. Carmen, *J. Appl. Phys.*, **99**, 084905 (2006).